# A Hybrid Control Method for Photovoltaic Grid-Connected Interleaved Flyback Micro-Inverter to Achieve High Efficiency in Wide Load Range*

Yue Zhang[1], Xiao-Fei He[2], Zhiliang Zhang[2], *Member, IEEE* and Yan-Fei Liu[3], *Senior Member IEEE*

[1]Jiangsu Electric Power Company Nanjing Power Supply Company
[2]Jiangsu Key Laboratory of New Energy Generation and Power Conversion
Nanjing University of Aeronautics andAstronautics, Nanjing, Jiangsu, P. R. China
[3]Department of Electrical and Computer Engineering
Queen's University, Kingston, Ontario, Canada, K7L 3N6
moon_zhang110@163.com, giftxiaofei@nuaa.edu.cn, zlzhang@nuaa.edu.cn and yanfei.liu@queensu.ca

***Abstract*— For flyback micro-inverters, Boundary Conduction Mode (BCM) and Discontinuous Conduction Mode (DCM) control strategies are widely used. Loss analysis is investigated for the interleaved flyback micro-inverter under BCM and DCM control strategies under different load condition. The BCM and DCM control strategies have different impact on the loss distribution and thus the efficiency of the flyback micro-inverter. Based on the loss analysis, a new hybrid control strategy combing the two-phase DCM and one-phase DCM control is proposed to improve the efficiency in wide load range by reducing the dominant losses depending on the load current. The experimental results verified the benefits of the proposed control.**

**Key words: Hybrid control, Micro-Inverter, Interleaved flyback**

## I. INTRODUCTION

Photovoltaic micro-inverter is recognized as an attractive solution for the residential utility-interactive PV system. Compared to the conventional centralized, string and multi-string inverters, micro-inverter has several advantages include more flexibility in system expansion, less installation cost, lower manufacturing cost through mass production, and higher maximum power point tracking (MPPT) efficiency [1].

The topologies of the single-phase grid-connected PV inverters are reviewed in [2]-[3]. The micro-inverter derived from the flyback converter, named as the flyback inverter, is widely used to its simple structure, lower cost and higher efficiency [4]. A single stage flyback inverter with the center-tapped secondary winding was presented in [5]. Each of the secondary winding transfers the energy to the AC side during a half line period with two additional MOSFETs. A modulated flyback DC/DC converter followed by a CSI was presented in [6]. The SCRs are used in the unfolding stage to reduce the cost and conduction loss. A dual mode switching strategy for the center-tapped secondary winding flyback inverter was presented in [6]-[8]. The BCM and DCM modulation methods were used simultaneously during a half line period, because BCM is suitable to high power levels and DCM is better for low power levels as far as the efficiency is concerned.

In this paper, the BCM and DCM control strategies are investigated of the interleaved flyback micro-inverter concentrating on the loss analysis under different load condition respectively. The advantages of two-phase DCM operation are the current sharing and the reduction of the current stress between two interleaved phases. On the other hand, the advantage of one-phase DCM operation is the reduction of the transformer core loss, the driving loss of the power MOSFETs. Therefore, two-phase DCM and one-phase DCM can be used simultaneously according to different output power during a half line period. Combining the two-phase DCM and one-phase DCM control, a new hybrid control method is proposed for the interleaved flyback micro-inverter to achieve high efficiency in wide load range. Moreover, the proposed control method is compatible with the digital implementation and requires no additional auxiliary circuitry.

## II. ANALYSIS OF FLYBACK INVERTER UNDER BCM AND DCM

### *A. Topology of the Interleaved Flyback Micro-Inverter*

Fig. 1 shows the main circuit of the interleaved flyback micro-inverter. Fig. 2 shows the principle of the micro-inverter. In interleaved flyback inverter, each phase is phase-shifted 180° for every switching cycle to achieve equivalent

*This work is supported by the Public Research Funding from Jiangsu Key laboratory of New Energy Generation and Power Conversion and the Technology Foundation for Selected Overseas Chinese Scholar from Ministry of the Industry and Information Technology.

double switching frequency and so to reduce the current ripple. The SCR bridge, which contains four SCRs, operates in the complementary mode at line frequency to change the polarity of output current filtered by filter inductor $L_f$ and capacity $C_f$. That means, the operation of interleaved flyback is exactly the same during each half line frequency period.

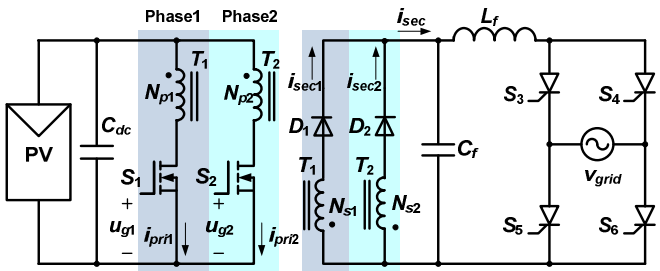


Fig. 1 Main circuit of the interleaved flyback micro-inverter

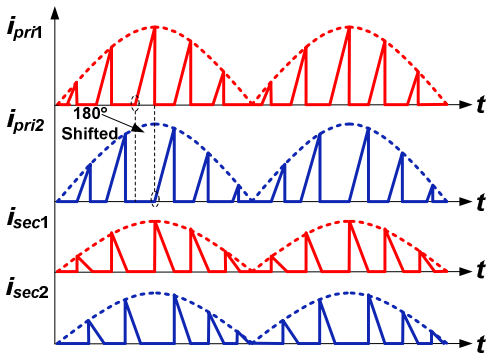


Fig. 2 Operation principle of the interleaved flyback micro-inverter

*B. Comparison of BCM and DCM*

The dominant losses with heavy load include the conduction loss of the MOSFETs and diodes, and the core loss and copper loss of the transformer, while the dominant losses with light load include the driving loss, turn-off loss of the MOSFETs and the transformer core loss. Under DCM, a Constant Switching Frequency (CSF) control is applied, while a Variable Switching Frequency (VSF) control is applied to achieve a sinusoidal waveform. The range of the switching frequency increases dramatically as the power level decreases for the flyback micro-inverter under BCM.

Fig. 3 shows the loss distribution comparison under BCM and DCM under half load condition. Fig. 4 shows the calculated efficiency of the interleaved flyback micro-inverter under DCM and BCM respectively. The specifications are as follows: input voltage $V_{dc}$=36~60 V; grid voltage: $V_g$=220 VAC; grid frequency: $f_{grid}$=50 Hz; switching frequency: $f_s$=100 kHz. The components of the power train are as follows: the transformer: $L_p$=28 μH, $L_s$=112 μH; $S_1$ and $S_2$: SPW52N50C3 (560 V/52 A from Infineon); $D_1$ and $D_2$: IDP12E120 (1200 V/12 A from Infineon); $S_3$-$S_6$: S8016N (800 V/16 A from Teccor). In this paper, the loss analysis is based on the above specifications.

It is noted that the turn off loss ($P_{off}$) and the gate driving loss ($P_{drive}$) under BCM are much higher than DCM due to the large switching frequency bandwidth of BCM. This translates into a significant reduction of the light load efficiency.

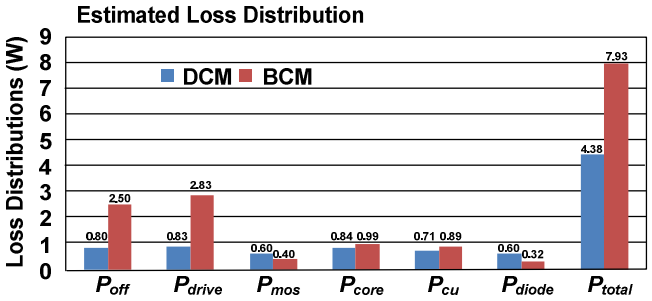


Fig. 3 Loss distribution under BCM and DCM: half load condition

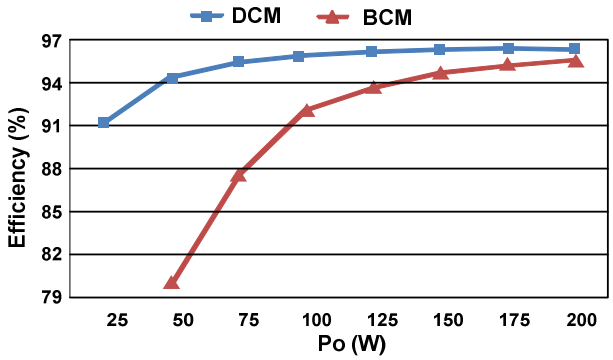


Fig. 4 Calculated efficiency comparison of BCM and DCM

## III. Proposed Hybrid Control Method and Priciple of Operation

*A. Loss Analysis of DCM*

Fig. 5 shows the calculated loss distribution of a 200 W interleaved flyback inverter under 100% and 25% load respectively. It is observed that the dominant losses with heavy load include the conduction loss of the power MOSFETs $P_{mos}$ and diodes $P_{diode}$, the transformer core loss $P_{core}$ and copper loss $P_{cu}$, whereas the dominant losses with light load include the gate driving loss $P_{drive}$, the turn-off loss $P_{off}$ of the power MOSFETs and the transformer core loss $P_{core}$. Therefore, minimizing the dominant losses according to load condition is an effective way to optimize the efficiency in wide load range.

For simplicity, 1Φ DCM represents only one phase operation and 2Φ DCM represents two phases operation under the interleaved mode. On the one hand, the 2Φ DCM operation shares the current and reduces the current stress between two interleaved phases. This is beneficial to reduce the conduction loss and turn-off loss of the power MOSFETs and diodes, as well as the copper loss of the transformer under heavy load condition. On the other hand, the 1Φ DCM operation minimizes the gate driving loss of the power MOSFETs as well as the core loss of the transformer under light load condition.

Based on the loss analysis, Fig. 6 shows the efficiency of the interleaved flyback inverter under 1Φ DCM and 2Φ DCM operation. It is noted that the efficiency improves while operating under 1Φ DCM within the power range of 105 W. Actually, 2Φ DCM and 1Φ DCM can be used simultaneously to modulate the interleaved flyback inverter depending on the load current during a half line period.

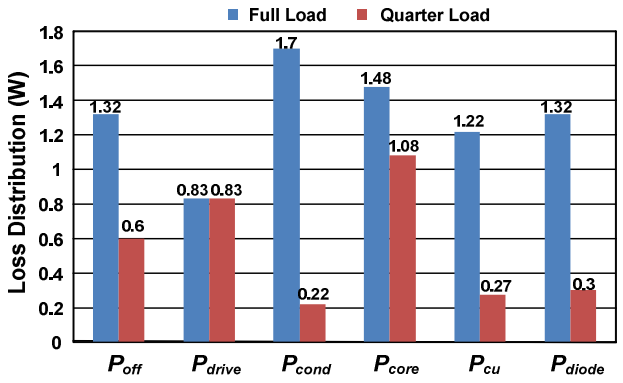


Fig. 5 Estimated Loss distribution of DCM under different load condition

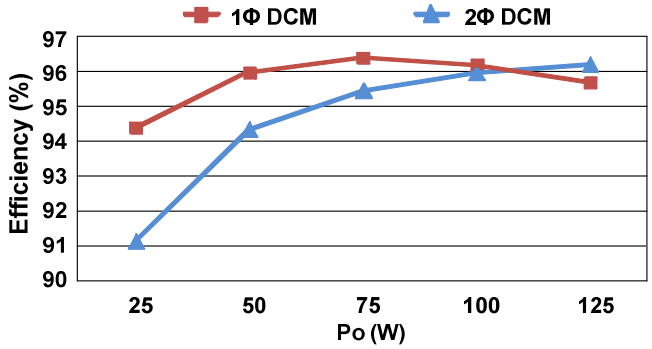


Fig. 6 Calculated efficiency of the micro-inverter under 1Φ DCM and 2Φ DCM

### B. Proposed Hybrid Control Method

The conventional DCM control only shuts down one phase when the load reduces to some power level. Actually, during the half line period, either 2Φ DCM or 1Φ DCM control can be applied. It is noticed that the output power $P_{out}$ during a half line period is a pulsating power following a squared sine wave. The output power $P_{out}$ in a half line period is

$$P_{out} = 2P_o \sin^2(\omega t) \tag{1}$$

where $P_o$ presents the average value of the output power delivered to the grid.

The idea here is to combine the advantages of 2Φ DCM and 1Φ DCM adaptively to the load current during a half line period with the phase shedding technology, so that the efficiency can be optimized in wide load range. Fig. 7 shows the operating region of 1Φ DCM and 2Φ DCM during a half line period.

In Fig. 7, 2Φ DCM is employed when load current is high and 1Φ DCM is employed when the load current under a certain level. Thus, the dominant losses are reduced depending on the load current and higher efficiency can be achieved in wide load range. Moreover, the proposed control is compatible with the digital implementation. It should be noted that as $P_o$ decreases, the 2Φ DCM region decreases simultaneously. In particular, when $P_o$ decreases to a certain level, the hybrid modulation merges into only 1Φ DCM.

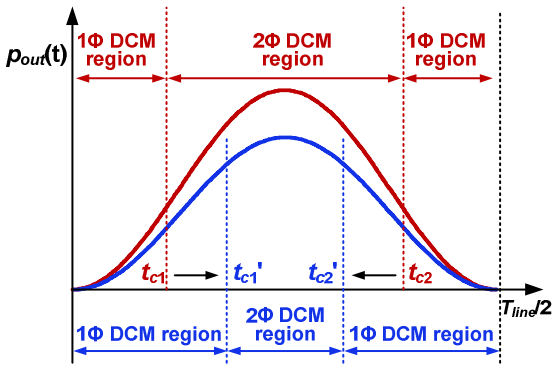


Fig. 7 Operation region of the 1Φ DCM and 2Φ DCM

### C. Design and Analysis of the Reference Signal

For the proposed control method, the reference signal $i_{ref}$ is used to generate the modulated duty cycles and needs to be well designed so that high efficiency and low THD can be achieved. Since the equivalent circuits of the two modules are similar, DCM of a single phase flyback inverter is analyzed firstly. Fig. 8 shows the equivalent circuit of the single flyback inverter during a half line period.

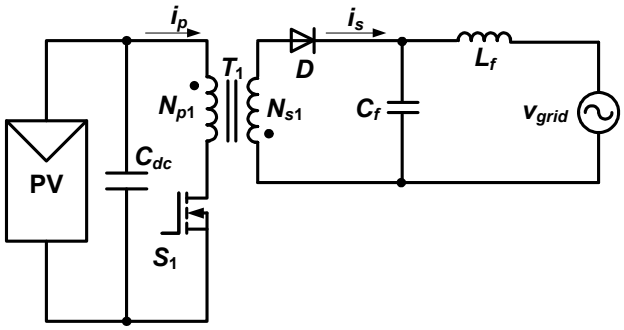


Fig. 8 Equivalent circuit of the single flyback inverter

During the $S_1$ on time, the primary current $i_p$ increases gradually in a linear relationship with the input voltage $V_{dc}$ and the primary inductance $L_p$. During the $S_1$ off time, the second current $i_s$ decreases in a linear relationship with the gird voltage $v_g$ $(t)$ and the secondary inductance $L_s$. The turn-on time $T_{on}$ and turn-off time $T_{off}$ in every switching period are

$$T_{on} = \frac{L_p \cdot I_p}{V_{dc}} \tag{2}$$

$$T_{off} = \frac{L_s \cdot I_s}{v_g(t)} \tag{3}$$

where $I_p$ and $I_s$ are the peak value of $i_p$ and $i_s$ in each switching period respectively. Since $I_p$ equals the reference signal $i_{ref}$, the relationships of $I_p$ and $I_s$ are

$$I_p = i_{ref} \tag{4}$$

$$I_s = I_p \cdot \sqrt{\frac{L_p}{L_s}} = i_{ref} \cdot \sqrt{\frac{L_p}{L_s}} \tag{5}$$

There is an approximation relationship as (6), where the RMS value of the output current $i_{out}$ equals the average value of $i_s$ in every switching period.

$$i_{out} = \frac{I_s \cdot T_{off}}{2T_s} \tag{6}$$

Considering the above equations, the relationship between $i_{out}$ and $i_{ref}$ is

$$i_{ref} = \sin(\omega t)\sqrt{\frac{2I_{out} \cdot V_o}{L_p \cdot f_s}} = 2\sin(\omega t)\sqrt{\frac{P_{o1}}{L_p \cdot f_s}} \tag{7}$$

where $I_{out}$ is the peak value of $i_{out}$; $V_o$ is the peak value of $v_g$ ($t$) and $P_{o1}$ is the average output power of each phase. For 2Φ DCM operation, $P_o$=2$P_{o1}$. The above equation can be rewritten as

$$i_{ref} = \sin(\omega t)\sqrt{\frac{2P_o}{L_p \cdot f_s}} \tag{8}$$

For the interleaved flyback micro-inverter with the proposed control method, the current reference $i_{ref1}$ and $i_{ref2}$ during a half line period are

$$i_{ref1} = \begin{cases} 2\sin(\omega t)\sqrt{\dfrac{P_o}{L_p \cdot f_s}} & (t < t_{c1}, t > t_{c2}) \\ \sin(\omega t)\sqrt{\dfrac{2P_o}{L_p \cdot f_s}} & (t_{c1} < t < t_{c2}) \end{cases} \tag{9}$$

$$i_{ref2} = \sin(\omega t)\sqrt{\frac{2P_o}{L_p \cdot f_s}} \quad (t_{c1} < t < t_{c2}) \tag{10}$$

As analyzed in Section III, the cross point of the efficiency curves under 2Φ DCM and 1Φ DCM is 105 W power level as illustrated in Fig. 6. For the convenience of calculation, 100 W is designed as an optimal boundary condition of 1Φ DCM and 2Φ DCM in this case. As a result, $t_{c1}$ and $t_{c2}$ can be obtained from (11) as shown in Fig. 7.

$$\sin(\omega t_{c1}) = \sin(\omega t_{c2}) = \sqrt{\frac{200}{4P_o}} = \sqrt{\frac{50}{P_o}} \tag{11}$$

### *D. Control Diagram of the Micro-Inverter*

Fig. 9 shows the control block diagram of the interleaved flyback inverter with the proposed control. The control blocks are implemented by Freescale DSP MC56F8257. In Fig. 9, Phase Locked Loop (PLL) is used to detect the phase angle, amplitude and frequency of the grid voltage. MPPT block is used to track the maximum power point of the PV panel.

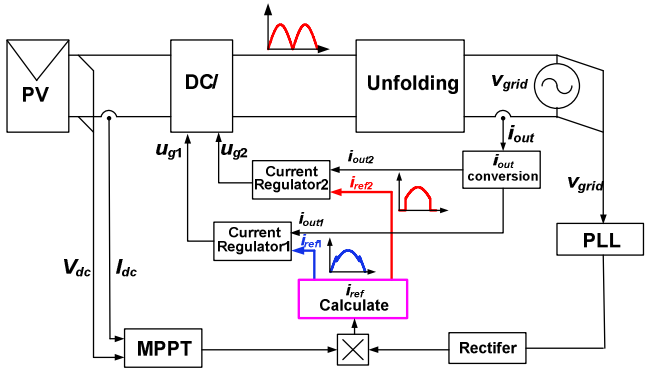


Fig. 9 Control diagram of the micro-inverter

## IV. Experimental Results and Discussion

To verify the proposed hybrid control method, a prototype of 200 W has been built. The specifications are the same as the analysis in Section V. A PV array simulator is used to verify the MPPT function of the proposed control. The major components used in the circuit are listed as follows: $S_1$ and $S_2$: SPW52N50C3; $D_1$ and $D_2$: IDP12E120; $S_3$-$S_6$: S8016N; the transformer: RM12, $L_P$=28 μH, $L_s$=112 μH, $L_k$=0.55 μH; the output filter inductance: $L_f$=600 μH; the output filter capacitor: $C_f$=0.33 μF.

The photo of prototype is illustrated in Fig. 10. A hall-effect sensor BJHCS-PS5 is used to sample the input current and an isolation amplifier HCPL-7840 is used to sample the input voltage. Therefore, the input power can be obtained. Two relays are used to achieve grid connection. A Freescale DSP MC56F8257 demo board is used to implement the proposed hybrid control.

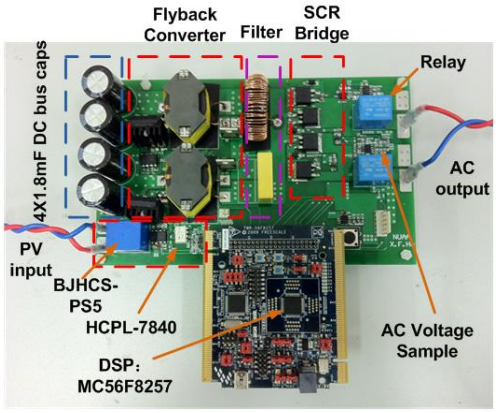


Fig. 10 Photo of the prototype

Fig. 11 shows the gate drive voltage and the primary current of phase 1 and phase 2 under different load condition. It is observed that as the power level decreases, the 2Φ DCM region decreases accordingly. When the power level decreases below 50 W, the hybrid modulation with 2Φ DCM and 1Φ DCM merges into only 1Φ DCM region as shown in Fig. 11 (c). This means the proposed control has the capability to achieve phase-shedding inherently.

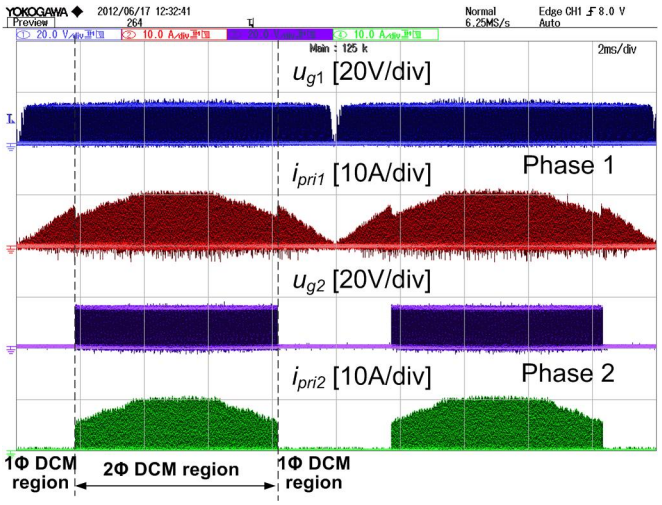


(a) Full load condition

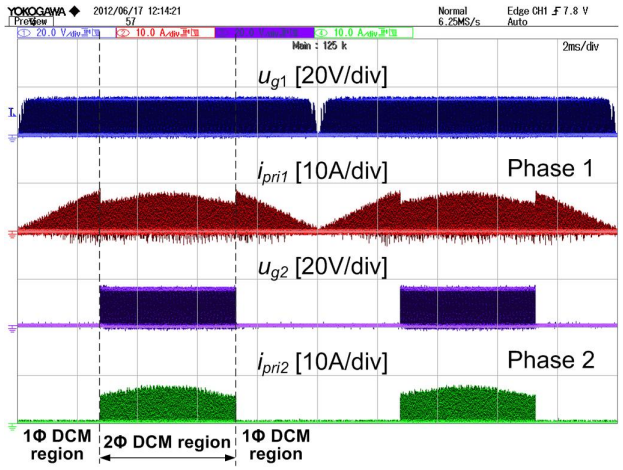


(b) Half load condition

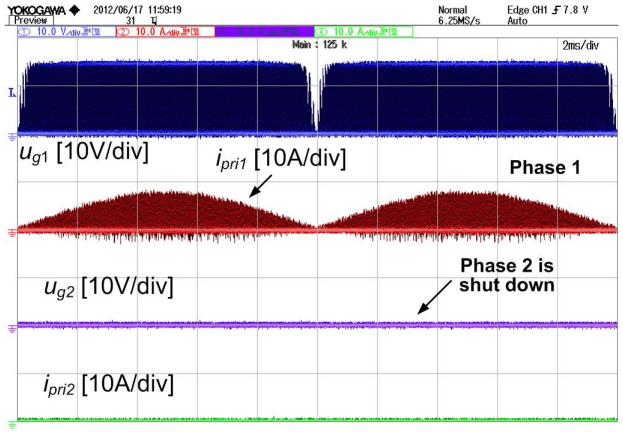


(c) Quarter load condition

Fig. 11 Gate drive voltage and primary current of Phase 1 and Phase 2 under different condition

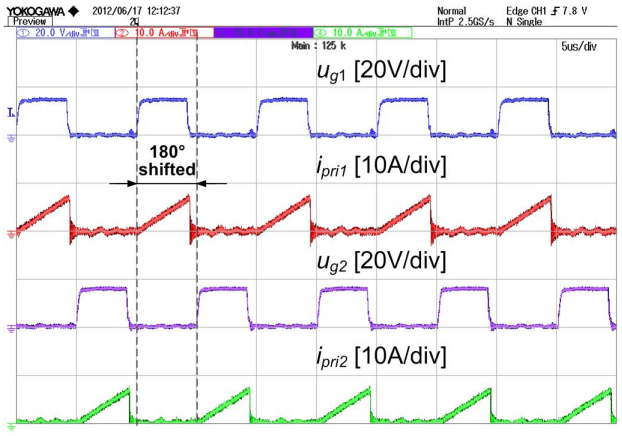


(b) Half load condition

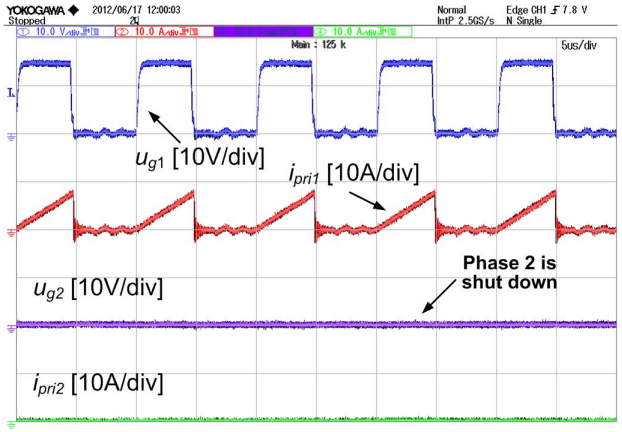


(c) Quarter load condition

Fig. 12 Gate drive voltage and primary current of Phase 1 and Phase 2 under different condition (expanded)

Fig. 12 shows the expanded waveforms of the gate drive voltage and the primary current of phase 1 and phase 2 under different load condition. From Fig. 12 (a) and Fig. 12 (b), the micro-inverter operates under the interleaved mode at 2Φ DCM region. Fig. 12 (c) shows that phase 2 is shut down when the power level decreases below 50 W.

Fig. 13 shows the gird voltage and output current under different load condition. The output current is able to catch up with the gird voltage with a sinusoidal waveform, and high power factor is achieved under different load condition.

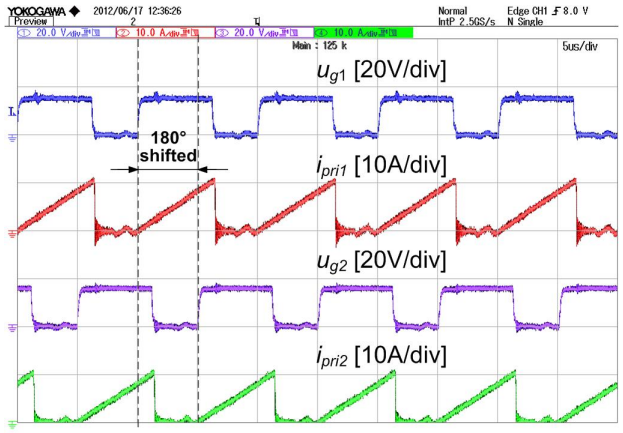


(a) Full load condition

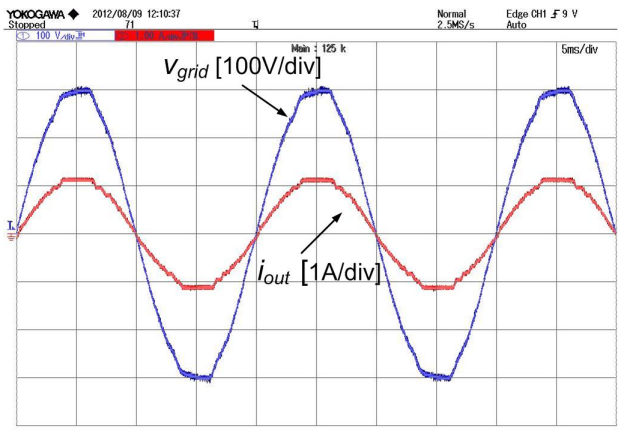


(a) Full load condition

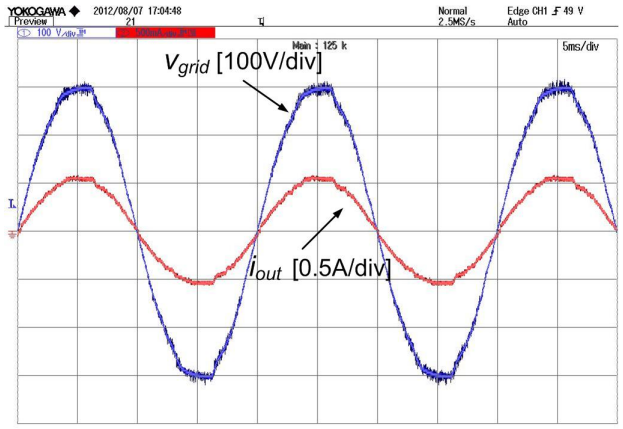


(b) Half load condition

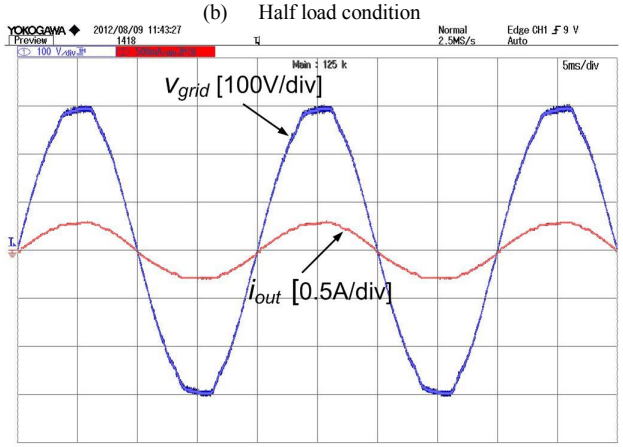


(c) Quarter Load condition

Fig. 13 Grid voltage and the output current

Fig. 14 shows the efficiency of the conventional control method and the proposed hybrid control method. With light load as $P_o$ is 50 W, the hybrid modulation with 2Φ DCM and 1Φ DCM merges into only 1Φ DCM region. The total loss of the micro-inverter is reduced by 1.8 W and the efficiency can be improved by 4% over the conventional two-phase interleaved mode. With heavy load as $P_o$ is 200 W, the 1Φ DCM region reduces and the loss reduction is 1.4 W, which translates into the efficiency improvement of 0.7%.

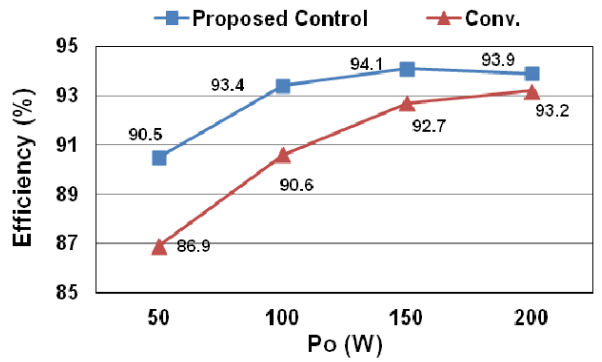


Fig. 14 Efficiency of conventional control and proposed hybrid control

## V. CONCLUSION

In this paper, the loss distribution and the efficiency of the interleaved flyback micro-inverter under BCM and DCM are investigated analytically under different power levels. It is found that DCM is a better choice than BCM within the power range of 200 W. For the interleaved flyback micro-inverter, the dominant losses with heavy load include the conduction loss of the power MOSFETs and diodes, and the core loss and copper loss of the transformer, while the dominant losses with light load include the gate driving loss, turn-off loss of the power MOSFETs and the transformer core loss. The 2Φ DCM operation shares the current and reduces the current stress between two interleaved phases. The conduction loss and turn off loss of the power MOSFETs and diodes and the copper loss of the transformer can be reduced at heavy load, and the 1Φ DCM reduces the driving loss of the main MOSFETs and the core loss of the transformer under light load condition. A new hybrid control strategy combining the 2Φ DCM and 1Φ DCM control during a half line period is proposed. With the proposed control strategy, high efficiency can be achieved in wide load range by reducing the dominant losses depending on the load current.

The experimental results verified the proposed control with the MPPT function. With the proposed control, the efficiency is improved around 4% under light load condition. Even under heavy load condition, the efficiency could be improved by 0.7%. Moreover, the proposed control method is compatible with the digital implementation and requires no additional auxiliary circuitry.

## REFERENCES


[1] W. Yu, C. Hutchens, J. S. Lai and T. Hegarty, "High efficiency converter with charge pump and coupled inductor for wide input photovoltaic AC module application," in *Proc. IEEE Energy Conversion Congress and Exposition*, 2009, pp. 3895-3900.

[2] S. B. Kjaer, J. K. Pedersen and F. Blaabjerg, "A review of single-phase grid-connected inverter for photovoltaic modules," *IEEE Trans. on Industry Applications*, Vol. 41, No. 5, pp. 1292-1306, Sep/Oct. 2005.

[3] Q. Li and P. Wolfs, "A Review of the single phase photovoltaic module integrated converter topologies with three different DC link configurations," *IEEE Trans. on Power Electronics*, Vol. 23, No. 3, pp. 1320-1333, May 2008.

[4] N. Kutkut and H. Hu, "Photovoltaic micro-inverters: topologies, control aspects, reliability issues, and applicable standards," in *Proc. IEEE Energy Conversion Congress and Exposition (ECCE)*, 2010, tutorial.

[5] A. C. Kyritsis, E .C. Tatakis and N. P. Papanikolaou, "Optimum design of the current-source flyback inverter for decentralized grid-connected photovoltaic systems," *IEEE Trans. on Energy Conversion*, Vol. 23, No. 1, pp. 281-293, March 2008.

[6] M. Gao, M. Chen, Q. Mo, Z. Qian and Y. Luo, "Research on output current of interleaved-flyback in boundary conduction mode for photovoltaic AC module application," in *Proc. IEEE Energy Conversion Congress and Exposition (ECCE)*, 2011, pp. 770-775.

[7] Y. H. Ji, D. Y. Jung, J. H. Kim, C. Y. Won and D. S. Oh, "Dual mode switching strategy of flybcak inverter for photovoltaic AC modules," in *Proc. IEEE Internationl Power Electronics Conference(IPEC)*, 2010, pp. 2924-2929.

[8] Z. Zhang, M. Chen, M. Gao, Q. Mo and Z. Qian, "An optimal control method for grid-connected photovoltaic micro-inverter to improve the efficiency at light-load condition," in *Proc. IEEE Energy Conversion Congress and Exposition (ECCE)*, 2011, pp. 219-224.